water

MDPI

Article

Evaluation and Development of Pedotransfer Functions and Artificial Neural Networks to Saturation Moisture Content Estimation

Josué Trejo-Alonso [1], Sebastián Fuentes [2], Nami Morales-Durán [3,4] and Carlos Chávez [2,*]

1 Engineering Faculty, Autonomous University of Queretaro, Cerro de las Campanas SN, Col. Las Campanas, Santiago de Querétaro 76010, Queretaro, Mexico
2 Water Research Center, Department of Irrigation and Drainage Engineering, Autonomous University of Queretaro, Cerro de las Campanas SN, Col. Las Campanas, Santiago de Querétaro 76010, Queretaro, Mexico
3 Chemical Sciencies Faculty, Autonomous University of Nuevo Leon, San Nicolas de los Garza 66451, Nuevo Leon, Mexico
4 Research Center for Biotechnology and Nanotechnology, Chemical Sciences Faculty, Research and Technological Innovation Park, Autonomous University of Nuevo Leon, Apodaca 66629, Nuevo Leon, Mexico
* Correspondence: chagcarlos@uaq.mx; Tel.: +52-442-192-1200 (ext. 6036)

Abstract: Modeling of irrigation and agricultural drainage requires knowledge of the soil hydraulic properties. However, uncertainty in the direct measurement of the saturation moisture content (θ_s) has been generated in several methodologies for its estimation, such as Pedotransfer Functions (PTFs) and Artificial Neuronal Networks (ANNs). In this work, eight different PTFs were developed for the (θ_s) estimation, which relate to the proportion of sand and clay, bulk density (BD) as well as the saturated hydraulic conductivity (K_s). In addition, ANNs were developed with different combinations of input and hidden layers for the estimation of θ_s. The results showed R^2 values from $0.9046 \leq R^2 \leq 0.9877$ for the eight different PTFs, while with the ANNs, values of $R^2 > 0.9891$ were obtained. Finally, the root-mean-square error (RMSE) was obtained for each ANN configuration, with results ranging from $0.0245 \leq RMSE \leq 0.0262$. It was found that with particular soil characteristic parameters (% Clay, % Silt, % Sand, BD and K_s), accurate estimate of θ_s is obtained. With the development of these models (PTFs and ANNs), high R^2 values were obtained for 10 of the 12 textural classes.

Keywords: soil hydraulic properties; artificial intelligence; soil water content; deficit irrigation

Citation: Trejo-Alonso, J.; Fuentes, S.; Morales-Durán, N.; Chávez, C. Evaluation and Development of Pedotransfer Functions and Artificial Neural Networks to Saturation Moisture Content Estimation. *Water* **2023**, *15*, 220. https://doi.org/10.3390/w15020220

Academic Editor: Paraskevi Londra

Received: 8 December 2022
Revised: 29 December 2022
Accepted: 29 December 2022
Published: 4 January 2023

1. Introduction

The physical soil parameters are essential in different studies related to the prediction of crop growth and irrigation efficiency, as well as the representation of the soil–water–plant–atmosphere relationship in the modeling of different irrigation methods and agricultural drainage [1–3].

The sustainable management of water resources has motivated the constant development of increasingly sophisticated models to describe water flow and solute transport in unsaturated soils [4]. These models are mainly based on the solution of the Richards equation [5] from the hydraulic conductivity curve $K(\psi)$ and the water retention curve $\theta(\psi)$. Both functions relate K and θ to the soil water potential (ψ). These two soil hydraulic properties (K and θ) are the key inputs to most models dealing with fitting the water transfer for different purposes [6,7]. Normally, the retention curve is estimated with the van Genuchten equation [8], which requires two shape parameters (m and n) estimated from the granulometric curve, and another three parameters related to soil moisture, characteristic pressure (ψ_d), residual moisture content (θ_r) and θ_s. The first parameter is calculated through the solution of the inverse problem with infiltration test data, while in most cases

$\theta_r = 0$ [9]. The parameter θ_s is one of the main parameters needed to find. the soil hydraulic characteristics.

The estimation of θ_s has been the focus of study by researchers in recent years, who have used direct and inverse techniques and methods to obtain this value. In general, the saturation moisture content can be obtained by several methods, including field measurement, land surface modeling, and remote sensing techniques [10]. Figure 1 shows a representative scheme for the main methods used to estimate the θ_s.

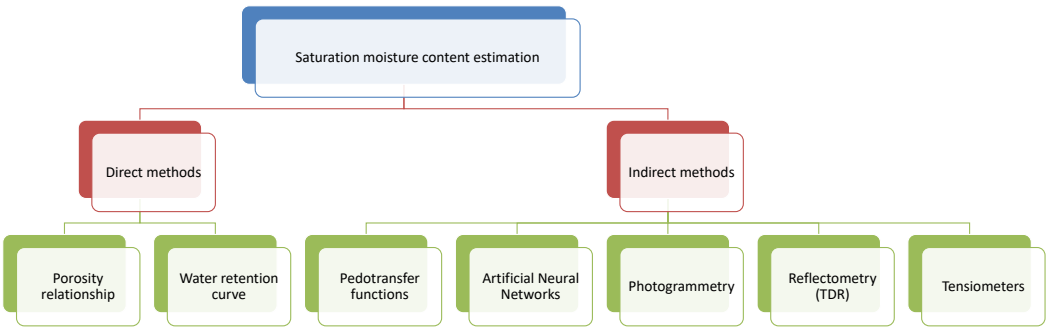

Figure 1. Main methods used in the saturation moisture content calculation.

The spatial information of saturation soil moisture data is obtained by active or passive remote sensing (photography and radar, respectively), which is a moisture estimation technique based on the use of geographic information systems and satellite information [11]. This technique requires both field and laboratory work to generate the correct soil moisture results. With remote sensing techniques, it is possible map the crops and their different characteristic parameters present in the soil [12–14]; these methods could be applied over large areas with low costs and with periodic observations [15,16].

Tensiometers are another method used in the field of agriculture to measure soil moisture and apply the necessary amount of water for the optimal development of the crops. A tensiometer consists of a porous cup, mainly ceramic with very fine pores, which is attached to a negative manometer by a plastic tube filled of water [17]. This method is widely used in drip [18] and sprinkler irrigation [19]. However, due to the fact that the instrument is outside, environmental and climatic conditions can easily damage it and generate erroneous measurements [20,21].

Using Time Domain Reflectometry (TDR) sensors is the most useful and non-destructive method used to determine the moisture content in soils and other porous means. This sensor measures the transmitted signal time from one end to the other [22,23]. However, in soils with high salt content, representativeness of the measurement can be lost, in addition to the fact that it requires a high initial investment [24].

Sensors in the field provide the most accurate estimates of soil moisture at different depths [25] however, in situ measurements are time-consuming and require specialized equipment that generates a high cost in the estimation of soil moisture.

The θ_s is the water volume in porous space, normally assimilated to the volumetric porosity (ϕ) by the following inequality $0 \leq \theta_s \leq \phi$; however, in saturated soil it takes $\theta_s = 0.9\phi$, which is due to the fact that a certain amount of air remains trapped in the porous medium [26,27]. Further, it is possible to consider $\theta_s = \phi$ as a simplification in the number of variables [28–30].

On the other hand, PTFs have been widely used to estimate soil properties in different geographic regions in response to the lack of data for soils, as well as the laborious, slow and expensive determination of the hydraulic properties [31,32]. Moreover, most PTFs are based on soil texture to predict and evaluate the retention curves [2,33–35]. Table 1 shows some PTFs published in the literature. The main similarity between them is the large number of necessary parameters in the θ_s estimation and most of them are either difficult to obtain in the laboratory or they present a high degree of complexity to calculate.

Table 1. PTFs for θ_s estimation.

PTF	Formula	Source
PTF1	$\theta_s = 0.81799 + 9.9 \times 10^{-4} \cdot \mathrm{Cl} - 0.3142 \cdot \mathrm{BD} + 1.8 \times 10^{-4} \cdot \mathrm{CEC} + 0.00451 \cdot \mathrm{pH} - 5 \times 10^{-6} \cdot \mathrm{Sa} \cdot \mathrm{Cl}$	[2]
PTF2	$\theta_s = 0.81 - 0.283 \cdot \mathrm{BD} + 0.001 \cdot \mathrm{Cl}$	[36]
PTF3	$\theta_s = 0.7019 + 0.001691 \cdot \mathrm{Cl} - 0.29619 \cdot \mathrm{BD} - 1.491 \times 10^{-6} \cdot \mathrm{Si}^2 + 8.21 \times 10^{-5} \cdot \mathrm{OM}^2 + 0.02427 \cdot \mathrm{Cl}^{-1} + 0.01113 \cdot \mathrm{Si}^{-1} + 0.01472 \ln(\mathrm{Si}) - 7.33 \times 10^{-5} \cdot \mathrm{OM} \cdot \mathrm{Cl} - 6.19 \times 10^{-4} \cdot \mathrm{BD} \cdot \mathrm{Cl} - 0.001183 \cdot \mathrm{BD} \cdot \mathrm{OM} - 1.664 \times 10^{-4} \cdot \mathrm{Si} \cdot \mathrm{tps}$	[37]

Notes: Abbreviations are as follows: Cl = Clay (% by weight); Si = Silt (% by weight); Sa = Sand (% by weight); BD = Bulk Density (Mg/m^3); OC = Organic Carbon (% by weight); OM = Organic Matter (% by weight); CEC = Cation Exchange Capacity (cmol/kg soil); pH (dimensionless); tps is the topsoil and is a qualitative variable having the value of 1.

Therefore, it is necessary to develop PTFs to estimate moisture by taking into account the largest amount parameters related to the soil and to obtain models that fit with the greatest possible precision to the in situ conditions presented in the majority agricultural crop plots.

In recent years, with the increasing progress in artificial intelligence, another alternative to PTFs has been explored: ANNs (e.g., [38] and references therein). ANNs are an artificial intelligence that simulate the behavior of the human brain, and their structures consist of a number of interconnected elements called neurons that are logically arranged in layers, which are denoted as input, output and hidden. Each neuron connects to all the neurons in the next layer via weighted connections. Erzin et al. [39] presents a detailed description of structure, functionality and configuration of ANNs.

Tomasella et al. [40] developed PTFs based on specific potential pressure points, from −4 to −1500 kPa. The advantage in the use of this technique is that it is possible to determine specific moisture points, such as θ_s. There are common functions such as the retention curve as Brooks and Corey [41] and van Genuchten [8], which require the characteristic soil parameters (θ_r, θ_s, ψ_d and n), where the n parameter represents the shape of the curve and ψ_d is a scale parameter. The uncertainty of these models increases with increasing clay content present in the analyzed soil [42] and, in some cases, the actual retention curve shape does not resemble the shape of the chosen equation for all available soil samples. Neural networks have been developed that have as their input parameter the natural logarithm of ψ; with this, it is possible to calculate the moisture content at the desired ψ, which varies with time [43]. Sand, silt and clay are the usual input parameters in the most common neural network models. In addition, it is possible to add the content of organic matter and bulk density as input parameters. Figure 2 shows a schematic representation of the three types of ANNs most used in the literature.

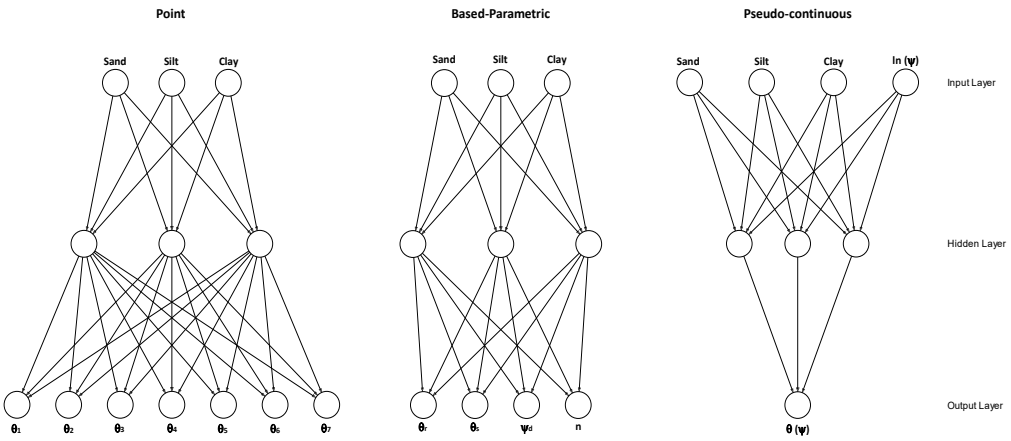

Figure 2. Schematic representation of principal types ANNs. Recovered from [43].

In surface irrigation modeling, the inflow discharge, the K_s and θ_s are the main factors that modify the irrigation depth applied to the crop. This is observed with infiltration

equations that take into account some soil parameters such as the Richards or the Green and Ampt equations, both with all their physically based parameters (e.g., [28–30,44]). The calculation of the optimal discharge necessary to obtain high values of the uniformity coefficient in surface irrigation is a function of the furrow or border length, hydrodynamic characteristics and moisture constants (initial and saturation moisture content) [45]. Therefore, it is important to develop efficient methodologies for the estimation of the θ_s parameter in order to make a correct design of surface irrigation and thus increase the water use efficiency.

The main goals in this work are: (a) to develop PTFs to estimate the θ_s, (b) to develop an artificial neural network, and (c) to compare the results of both models between them and with other works in the literature.

2. Materials and Methods

2.1. Study Area

The database used in this study was developed from samplings in 900 plots in the Irrigation District 023 located between the municipalities of San Juan del Rio and Pedro Escobedo in the state of Queretaro, Mexico and has an area of 11,048 ha.

The bulk density was determined by the cylinder method of known volume, the soil texture by the mesh analysis and the Bouyoucos hydrometer [46], the initial water content through a TDR 300 soil moisture meter, and field capacity (−33 kPa) and permanent wilting point (−1500 kPa) were measured in a pressure plate [47], while K_s was obtained by the variable head permeameter method. The measurement of variables and the hydrodynamic characterization of soils are widely discussed in [48,49].

2.2. Soil Textures

Soil texture is an indicator of the amount of water that soil can store and, consequently, the irrigation interval with which crops must be watered. Figure 3 shows the texture classification obtained from the laboratory and classified according to the triangle of textures proposed by the USDA using the R package "soil texture" [50]. This texture is determined by the proportion of sand, silt and clay and according to the triangle.

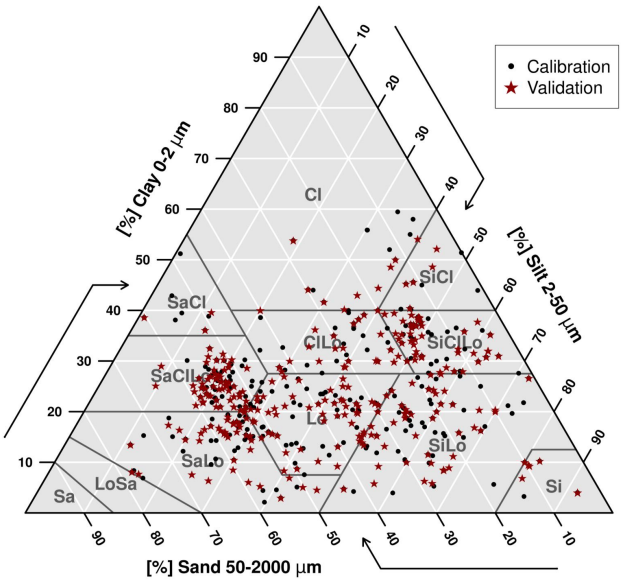

Figure 3. Distribution of soil textures for calibration (450 points) and validation (450 points) data. Abbrevations are as follows: clay (Cl), sand (Sa), silt (Si), loam (Lo), sandy clay (SaCl), silty clay (SiCl), sandy clay loam (SaClLo), clay loam (ClLo), silty clay loam (SiClLo), sandy loam (SaLo), silty loam (SiLo) and loamy sand (LoSa).

2.3. Statistical Analysis

The PTFs' confiability depends on factors that were not considered as predictors, such as the soil characteristics, climatic conditions, landscape characteristics and geographical regions of the soils.

The most used statistic indicators to evaluate the goodness of fit of the PTFs are the root-mean-square error (RMSE), the mean error (ME) and the correlation coefficient (R^2) [51,52].

$$\mathrm{RMSE} = \sqrt{\frac{1}{N}\sum_{i=1}^{N}(E_i - M_i)^2} \quad (1)$$

$$\mathrm{ME} = \frac{1}{N}\sum_{i=1}^{N}(E_i - M_i) \quad (2)$$

$$\mathrm{R}^2 = 1 - \frac{\sum_{i=1}^{N}(M_i - E_i)^2}{\sum_{i=1}^{N}(M_i - \bar{M})^2} \quad (3)$$

where M_i is the value measured in the field, E_i is the estimated value, $\bar{M}$ is the measured values' mean, i is the i-th value of the measured or estimated data and N is the total number of data points for each soil sample .

The small and homogeneous databases tend to produce better error metrics (RMSE, ME, R^2) than bigger databases, which include a significant variability in the soil type, porosity and texture [53].

2.4. Development of the PTFs and the ANNs

Based on the study of Trejo-Alonso et al. [54], eight new PTFs were developed based on the results of a Principal Component Analysis (PCA). This decision was made due to the fact that only the PTF published by Vereecken et al. [36] could be tested and the lack of PTFs for θ_s in the literature.

For the new PTFs, we shouldonly consider the next variables from the database: % Clay, % Sand, BD and K_s. The PTFs and the plots in this work were constructed using R software [55], and 450 random values are used for calibration and 450 for validation.

For the ANNs, the "neuralnet" package [56] and the "caret" package [57], provided by the R software, were used with 75% of the sample for training and 25% for validation. Two different ANNs were constructed, the first one with four input data points (% Clay, % Silt, BD and K_s) and the second one with five input data points (% Clay, % Silt, % Sand, BD and K_s). Two hidden layers were maintained in both ANNs, and the number of neurons in each layer varies from 2 to 10. This process led to 81 ANN configurations and, finally, the two best configurations were selected.

3. Results

3.1. PTFs

The dominating soil texture in this region is SiClLo (18.11%), followed by SiLo (16.11%) which can be observed in Figure 3. With the determination of this soil property, it is possible to detect plots where irrigation depths and irrigation times were excessive [28].

Figure 4 shows the new PTFs constructed in this study, and Table 2 shows the mathematical expressions. Models with silt percentage data were tested too, but with worse or very similar results. This was already indicated by the PCA analysis.

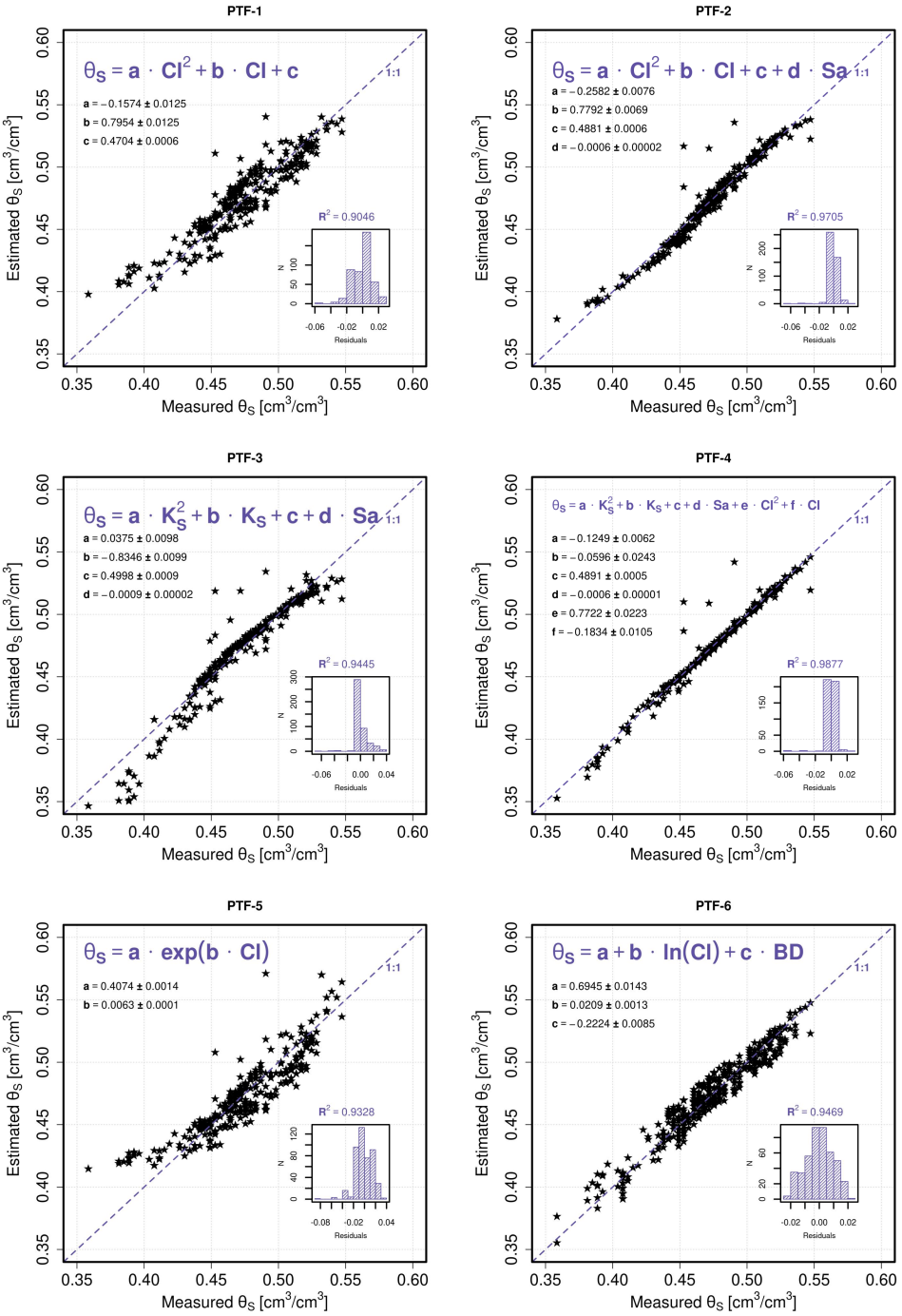

Figure 4. *Cont.*

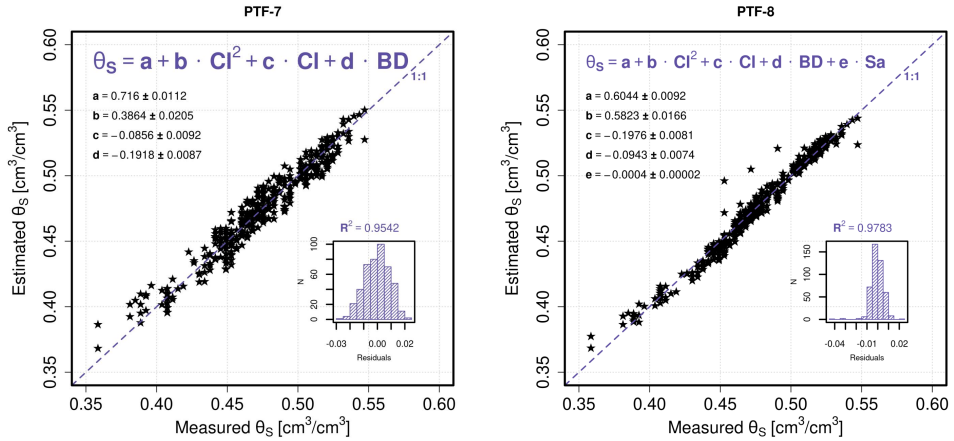

Figure 4. Comparison between the measured θ_s and the estimated one by the PTF. The PTF equations are at the top left, and the values for each constant are below that. In addition, the R^2 value and a residual histogram are available.

Table 2. New pedotransfer functions.

PTF	Formula	R^2
PTF-1	$\theta_s = a \cdot Cl^2 + b \cdot Cl + c$	0.9046
PTF-2	$\theta_s = a \cdot Cl^2 + b \cdot Cl + c + d \cdot Sa$	0.9705
PTF-3	$\theta_s = a \cdot K_s^2 + b \cdot K_s + c + d \cdot Sa$	0.9445
PTF-4	$\theta_s = a \cdot K_s^2 + b \cdot K_s + c + d \cdot Sa + e \cdot Cl^2 + f \cdot Cl$	0.9877
PTF-5	$\theta_s = a \cdot \exp(b \cdot Cl)$	0.9328
PTF-6	$\theta_s = a + b \cdot \ln(Cl) + c \cdot BD$	0.9469
PTF-7	$\theta_s = a + b \cdot Cl^2 + c \cdot Cl + d \cdot BD$	0.9542
PTF-8	$\theta_s = a + b \cdot Cl^2 + c \cdot Cl + d \cdot BD + e \cdot Sa$	0.9783

Notes: Abbreviations are as follows: Cl = Clay (% by weight); Sa = Sand (% by weight); BD = Bulk Density (g/cm^3); K_s (cm/h) and the coefficients from a to f are obtained by fitting the model to the experimental data.

3.2. ANN

The best configuration for the ANN with four input layers was 4-9-10-1, which means four inputs, nine neurons in the first hidden layer, ten neurons in the second hidden layer and one output. For the five input layers, a 5-10-10-1 configuration was implemented. The main results of these two ANNs are summarized in Table 3. The results obtained provided high R^2, which could be considered satisfactory when compared to other studies [2,36,37].

Table 3. ANN results.

ANN	RMSE	R^2	ME
4-9-10-1	0.0182	0.9891	0.0091
5-10-10-1	0.0195	0.9903	0.0095

Figure 5 shows the main results of the ANN constructions process. Figure 6 shows the ANN implementation in the validation data.

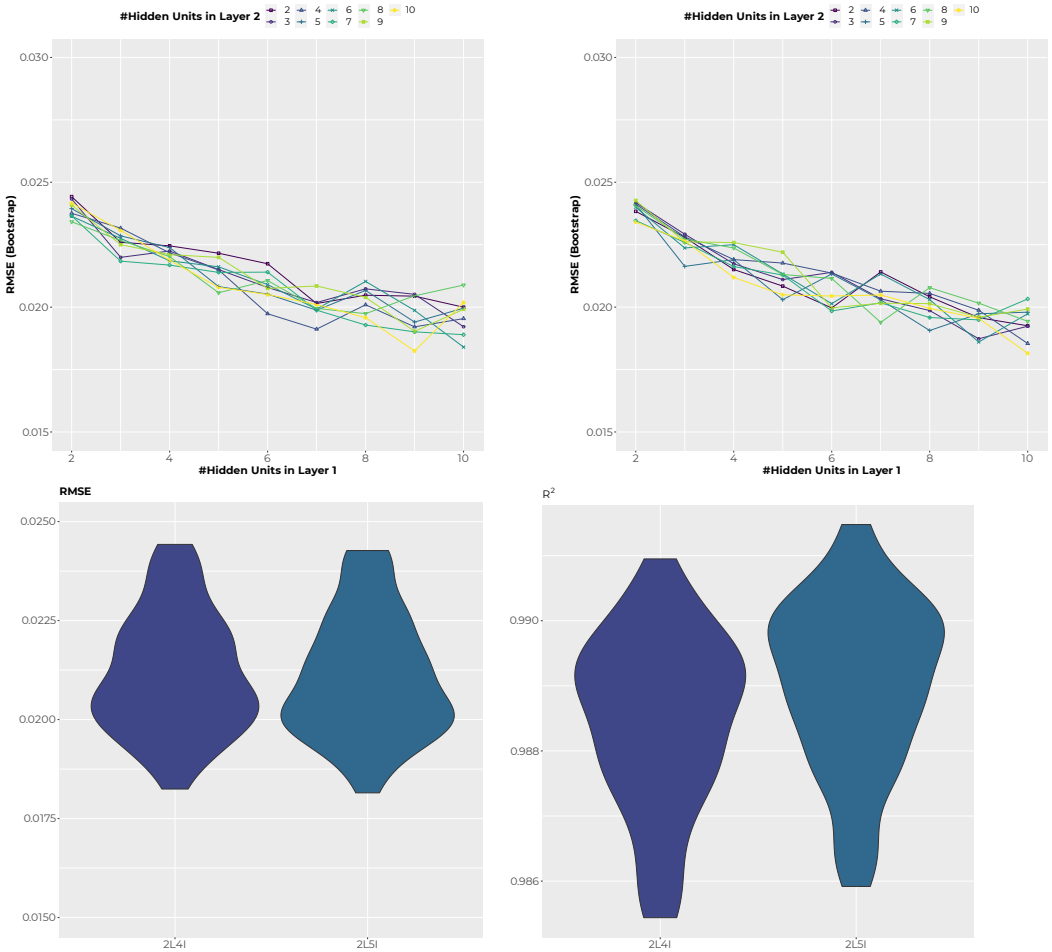

Figure 5. Results for the 81 ANN configurations. (**Top**) The RMSE variations for each ANN configuration. (**Bottom**) Statistical analysis (RMSE and R^2) for each ANN configuration; 2L4I means two layers and four input parameters, while 2L5I is two layers and five input data points.

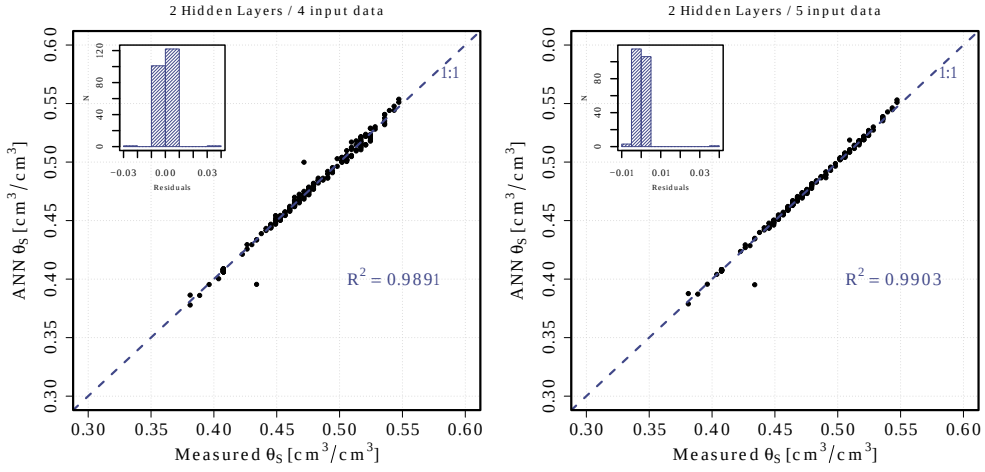

Figure 6. Results for the 4-9-10-1 (**left**) and 5-10-10-1 (**right**) configuration predictions applied in the validation data.

4. Discussion

In this work, it has been proved that ANNs are more precise than PTFs in the θ_s modeling with better values in R^2 even with the most simple ANN (four input parameters).

Furthermore, for comparative purposes, the results obtained with the studies mentioned in Table 2 were analyzed. Hodnett and Tomasella [2] found θ_s values from 0.4100 to 0.6010 cm^3/cm^3; meanwhile, the sample θ_s values here obtained ranged from 0.3500 to 0.5500 cm^3/cm^3. This difference is explained by the fact that the soil samples used in this study come from cultivated areas and cover 10 of 12 textural classes. In addition, Hodnett and Tomasella [2] used six input parameters and only linear relations for the PTF construction, and the R^2 or RMSE information was missing. In this work, only four parameters were used for the more complex calculated TFP, and nonlinear relationships were constructed. In this case, no data on organic matter content were available; therefore, it was not possible to test the PTF found by Hodnet and Tomasella [2]. Vereecken et al. [36] used 182 samples from the north of the Samber and Meuse rivers, Belgium, in which they concluded that θ_s can be estimated with two soil properties (bulk density and clay content), obtaining an $R^2 = 0.8480$. Finally, Wösten et al. [37] used the HYPRES database, which contains information on a total of 5521 soil horizons, to create a PTF of θ_s from only 4030 soil horizons, including six input variables, where horizon depth stands out as a quantitative variable. However, even having used all this information, they obtained an $R^2 = 0.7600$ due to the absence of some hydraulic properties such as K_s. Despite exploring nonlinear forms for PTFs, the result found by Vereecken et al. [36] present the same problem as Wösten et al. [37], where both use bulk density and clay content as input data; $R^2 < 0.8500$ is observed.

Therefore, eight new PTFs were found that proved to be more accurate compared to those found in the literature for the calculation of θ_s. The models here developed present the advantage of having a high value of R^2 and the characteristic of only requiring three primary soil variables as the input parameter, which are clay and sand content, as well as K_s in two of the eight functions or BD in three of the eight functions developed.

Furthermore, with the development of ANNs with the same four input parameters, it is shown that the error obtained in the PTFs can be reduced.

The development of PTFs is a useful tool that can be applied mainly in irrigation (sprinkler, drip or surface), as well as in agricultural drainage, to estimate soil parameters that are difficult to access. They are easy to evaluate and depend on the number of variables to be applied. However, ANN is an alternative when a more accurate approximation is sought, as long as computer equipment (hardware and software) is not a disadvantage.

5. Conclusions

In this work, eight new PTFs were developed for θ_s estimation, considering the clay and sand content (%), BD (g/cm^3) and the K_s (cm/h), based on 900 samples. The results showed, for PTFs, $R^2 > 0.9046$, reaching a maximum value of $R^2 = 0.9877$, where only three input parameters were used. These functions can be used to offer a quick response in the irrigation modeling and drainage, but with a high capacity of improvement to obtain an optimal design.

Further, 81 artificial neural networks were constructed and tested to calculate the θ_s, based on the best RMSE values. Two of them were selected as the final ANNs, the first one with four input data and the second one with five. The results showed $R^2 > 0.9891$, which suggests that the use of the ANN is necessary to develop more accurate designs in the irrigation models, which show better results in the final parameter estimations.

Author Contributions: J.T.-A., S.F., N.M.-D. and C.C. contributed equally to this work. All authors have read and agreed to the published version of the manuscript.

Funding: This research was supported as part of a collaboration between the National Water Commission (CONAGUA, according to its Spanish acronym); the Irrigation District 023, San Juan del Rio, Queretaro; and the Autonomous University of Queretaro, under the program RIGRAT 2015–2019.

Institutional Review Board Statement: Not applicable.

Informed Consent Statement: Not applicable.

Data Availability Statement: Not applicable.

Acknowledgments: We would like to thank the academic editor and the expert reviewers for their detailed comments and suggestions for the manuscript. These were very helpful in improving the quality of the manuscript.

Conflicts of Interest: The authors declare no conflict of interest.

References

1. Shelia, V.; Šimůnek, J.; Boote, K.; Hoogenbooom, G. Coupling DSSAT and HYDRUS-1D for Simulations of Soil Water Dynamics in the Soil-Plant-Atmosphere System. *J. Hydrol. Hydromech.* **2018**, *66*, 232–245. [CrossRef]
2. Hodnett, M.G.; Tomasella, J. Marked Differences between van Genuchten Soil Water-Retention Parameters for Temperate and Tropical Soils: A New Water-Retention Pedo-Transfer Functions Developed for Tropical Soils. *Geoderma* **2002**, *108*, 155–180. [CrossRef]
3. Tian, H.; Huang, N.; Niu, Z.; Qin, Y.; Pei, J.; Wang, J. Mapping Winter Crops in China with Multi-Source Satellite Imagery and Phenology-Based Algorithm. *Remote Sens.* **2019**, *11*, 820. [CrossRef]
4. Schaap, M. Using Neural Networks to Predict Soil Water Retention and Soil Hydraulic Conductivity. *Soil Tillage Res.* **1998**, *47*, 37–42. [CrossRef]
5. Richards, L.A. Capillary Conduction of Liquids through Porous Mediums. *Physics* **1931**, *1*, 318–333. [CrossRef]
6. Balland, V.; Pollacco, J.A.P.; Arp, P.A. Modeling Soil Hydraulic Properties for a Wide Range of Soil Conditions. *Ecol. Model.* **2008**, *219*, 300–316. [CrossRef]
7. Wösten, J.H.M.; Verzandvoort, S.J.E.; Leenaars, J.G.B.; Hoogland, T.; Wesseling, J.G. Soil Hydraulic Information for River Basin Studies in Semi-Arid Regions. *Geoderma* **2013**, *195–196*, 79–86. [CrossRef]
8. Van Genuchten, M.T. A Closed-Form Equation for Predicting the Hydraulic Conductivity of Unsaturated Soils. *Soil Sci. Soc. Am. J.* **1980**, *44*, 892–898. [CrossRef]
9. Zavala, M.; Fuentes, C.; Saucedo, H. On the radiation condition in the drainage of an initially saturated soil column. *Ing. Hidraul. Mex.* **2003**, *18*, 121–131.
10. Liang, S.; Wang, J. *Advanced Remote Sensing: Terrestrial Information Extraction and Applications*; Academic Press: Cambridge, MA, USA, 2019; ISBN 978-0-12-815826-5.
11. Ahlmer, A.-K.; Cavalli, M.; Hansson, K.; Koutsouris, A.J.; Crema, S.; Kalantari, Z. Soil Moisture Remote-Sensing Applications for Identification of Flood-Prone Areas along Transport Infrastructure. *Environ. Earth Sci.* **2018**, *77*, 533. [CrossRef]
12. Qiu, B.; Luo, Y.; Tang, Z.; Chen, C.; Lu, D.; Huang, H.; Chen, Y.; Chen, N.; Xu, W. Winter Wheat Mapping Combining Variations before and after Estimated Heading Dates. *ISPRS J. Photogramm. Remote Sens.* **2017**, *123*, 35–46. [CrossRef]
13. Atzberger, C. Advances in Remote Sensing of Agriculture: Context Description, Existing Operational Monitoring Systems and Major Information Needs. *Remote Sens.* **2013**, *5*, 949–981. [CrossRef]
14. Yuping, M.; Shili, W.; Li, Z.; Yingyu, H.; Liwei, Z.; Yanbo, H.; Futang, W. Monitoring Winter Wheat Growth in North China by Combining a Crop Model and Remote Sensing Data. *Int. J. Appl. Earth Obs. Geoinf.* **2008**, *10*, 426–437. [CrossRef]
15. He, L.; Song, X.; Feng, W.; Guo, B.-B.; Zhang, Y.-S.; Wang, Y.-H.; Wang, C.-Y.; Guo, T.-C. Improved Remote Sensing of Leaf Nitrogen Concentration in Winter Wheat Using Multi-Angular Hyperspectral Data. *Remote Sens. Environ.* **2016**, *174*, 122–133. [CrossRef]
16. Franke, J.; Menz, G. Multi-Temporal Wheat Disease Detection by Multi-Spectral Remote Sensing. *Precis. Agric.* **2007**, *8*, 161–172. [CrossRef]
17. Aziz, M.; Khan, M.; Anjum, N.; Sultan, M.; Shamshiri, R.R.; Ibrahim, S.M.; Balasundram, S.K.; Aleem, M. Scientific Irrigation Scheduling for Sustainable Production in Olive Groves. *Agriculture* **2022**, *12*, 564. [CrossRef]
18. Zapata-Sierra, A.; Roldán-Cañas, J.; Reyes-Requena, R.; Moreno-Pérez, M. Study of the Wet Bulb in Stratified Soils (Sand-Covered Soil) in Intensive Greenhouse Agriculture under Drip Irrigation by Calibrating the Hydrus-3D Model. *Water* **2021**, *13*, 600. [CrossRef]
19. Koumanov, K.S.; Hopmans, J.W.; Schwankl, L.J.; Andreu, L.; Tuli, A. Application Efficiency of Micro-Sprinkler Irrigation of Almond Trees. *Agric. Water Manag.* **1997**, *34*, 247–263. [CrossRef]
20. Butters, G.L.; Cardon, G.E. Temperature Effects on Air-Pocket Tensiometers. *Soil Sci.* **1998**, *163*, 677–685. [CrossRef]
21. Warrick, A.W.; Wierenga, P.J.; Young, M.H.; Musil, S.A. Diurnal Fluctuations of Tensiometric Readings Due to Surface Temperature Changes. *Water Resour. Res.* **1998**, *34*, 2863–2869. [CrossRef]
22. He, H.; Aogu, K.; Li, M.; Xu, J.; Sheng, W.; Jones, S.B.; González-Teruel, J.D.; Robinson, D.A.; Horton, R.; Bristow, K.; et al. A. Review of Time Domain Reflectometry (TDR) Applications in Porous Media. *Adv. Agron.* **2021**, *168*, 83–155.
23. Noborio, K. Measurement of Soil Water Content and Electrical Conductivity by Time Domain Reflectometry: A Review. *Comput. Electron. Agric.* **2001**, *31*, 213–237. [CrossRef]
24. Rasheed, M.W.; Tang, J.; Sarwar, A.; Shah, S.; Saddique, N.; Khan, M.U.; Imran Khan, M.; Nawaz, S.; Shamshiri, R.R.; Aziz, M.; et al. Soil Moisture Measuring Techniques and Factors Affecting the Moisture Dynamics: A Comprehensive Review. *Sustainability* **2022**, *14*, 11538. [CrossRef]

25. Zhang, Y.; Liang, S.; Zhu, Z.; Ma, H.; He, T. Soil Moisture Content Retrieval from Landsat 8 Data Using Ensemble Learning. *ISPRS J. Photogramm. Remote Sens.* **2022**, *185*, 32–47. [CrossRef]
26. Haverkamp, R.; Debionne, S.; Viallet, P.; Angulo-Jaramillo, R.; de Condappa, D.; Delleur, J.W. Soil Properties and Moisture Movement in the Unsaturated Zone. In *The Handbook of Groundwater Engineering*; CRC Press: Boca Raton, FL, USA, 2006; pp. 1–59.
27. Rogowski, A.S. Watershed Physics: Model of the Soil Moisture Characteristic. *Water Resour. Res.* **1971**, *7*, 1575–1582. [CrossRef]
28. Chávez, C.; Fuentes, C. Design and Evaluation of Surface Irrigation Systems Applying an Analytical Formula in the Irrigation District 085, La Begoña, Mexico. *Agric. Water Manag.* **2019**, *221*, 279–285. [CrossRef]
29. Saucedo, H.; Zavala, M.; Fuentes, C. Border irrigation design with the Saint-Venant and Green & Ampt equations. *Water Technol. Sci.* **2015**, *6*, 103–112.
30. Fuentes, S.; Fuentes, C.; Saucedo, H.; Chávez, C. Border Irrigation Modeling with the Barré de Saint-Venant and Green and Ampt Equations. *Mathematics* **2022**, *10*, 1039. [CrossRef]
31. Patil, N.G.; Singh, S.K. Pedotransfer Functions for Estimating Soil Hydraulic Properties: A Review. *Pedosphere* **2016**, *26*, 417–430. [CrossRef]
32. Botula, Y.-D.; Van Ranst, E.; Cornelis, W.M. Pedotransfer Functions to Predict Water Retention for Soils of the Humid Tropics: A Review. *Rev. Bras. Ciênc. Solo*. **2014**, *38*, 679–698. [CrossRef]
33. Botula, Y.-D.; Cornelis, W.M.; Baert, G.; Van Ranst, E. Evaluation of Pedotransfer Functions for Predicting Water Retention of Soils in Lower Congo (D.R. Congo). *Agric. Water Manag.* **2012**, *111*, 1–10. [CrossRef]
34. Santra, P.; Kumar, M.; Kumawat, R.N.; Painuli, D.K.; Hati, K.M.; Heuvelink, G.B.M.; Batjes, N.H. Pedotransfer Functions to Estimate Soil Water Content at Field Capacity and Permanent Wilting Point in Hot Arid Western India. *J. Earth Syst. Sci.* **2018**, *127*, 35. [CrossRef]
35. Lee, K.-S.; Lee, D.-S.; Jung, H.-G.; Lee, S.-P.; Ryu, J.-H.; Choi, W.-J.; Yang, J.-E.; Chung, D.-Y. Evaluation of Pedotransfer Functions for Estimating Soil Water Retention Curve of Ap Horizon Soils for Various Soil Series of Reclaimed Tidal Flat Soil. *Agronomy* **2022**, *12*, 1507. [CrossRef]
36. Vereecken, H.; Maes, J.; Feyen, J.; Darius, P. Estimating the soil moisture retention characteristic from texture, bulk density, and carbon content. *Soil Sci.* **1989**, *148*, 389–403. [CrossRef]
37. Wösten, J.H.M.; Pachepsky, Ya.A.; Rawls, W.J. Pedotransfer Functions: Bridging the Gap between Available Basic Soil Data and Missing Soil Hydraulic Characteristics. *J. Hydrol.* **2001**, *251*, 123–150. [CrossRef]
38. Trejo-Alonso, J.; Fuentes, C.; Chávez, C.; Quevedo, A.; Gutierrez-Lopez, A.; González-Correa, B. Saturated Hydraulic Conductivity Estimation Using Artificial Neural Networks. *Water* **2021**, *13*, 705. [CrossRef]
39. Erzin, Y.; Gumaste, S.D.; Gupta, A.K.; Singh, D.N. Artificial neural network (ANN) models for determining hydraulic conductivity of compacted fine-grained soils. *Can. Geotech. J.* **2009**, *46*, 955–968. [CrossRef]
40. Tomasella, J.; Pachepsky, Y.; Crestana, S.; Rawls, W.J. Comparison of Two Techniques to Develop Pedotransfer Functions for Water Retention. *Soil Sci. Soc. Am. J.* **2003**, *67*, 1085–1092. [CrossRef]
41. Brooks, R.H.; Corey, A.T. Hydraulic Properties of Porous Media and Their Relation to Drainage Design. *Trans. ASAE*. **1964**, *7*, 26–28. [CrossRef]
42. Børgesen, C.D.; Schaap, M.G. Point and Parameter Pedotransfer Functions for Water Retention Predictions for Danish Soils. *Geoderma* **2005**, *127*, 154–167. [CrossRef]
43. Haghverdi, A.; Cornelis, W.M.; Ghahraman, B. A Pseudo-Continuous Neural Network Approach for Developing Water Retention Pedotransfer Functions with Limited Data. *J. Hydrol.* **2012**, *442–443*, 46–54. [CrossRef]
44. Bautista, E.; Schlegel, J.L.; Clemmens, A.J. The SRFR 5 Modeling System for Surface Irrigation. *J. Irrig. Drain Eng.* **2016**, *142*, 04015038. [CrossRef]
45. Fuentes, C.; Chávez, C. Analytic Representation of the Optimal Flow for Gravity Irrigation. *Water* **2020**, *12*, 2710. [CrossRef]
46. Bouyoucos, G.J. Hydrometer Method Improved for Making Particle Size Analyses of Soils. *Agron. J.* **1962**, *54*, 464–465. [CrossRef]
47. Richards, L.A.; Fireman, M. Pressure-Plate Apparatus for Measuring Moisture Sorption and Transmission by Soils. *Soil Sci.* **1943**, *56*, 395–404. [CrossRef]
48. Chávez, C.; Fuentes, S.; Fuentes, C.; Brambila-Paz, F.; Trejo-Alonso, J. How Surface Irrigation Contributes to Climate Change Resilience—A Case Study of Practices in Mexico. *Sustainability* **2022**, *14*, 7689. [CrossRef]
49. Chávez, C.; Limón-Jiménez, I.; Espinoza-Alcántara, B.; López-Hernández, J.A.; Bárcenas-Ferruzca, E.; Trejo-Alonso, J. Water-Use Efficiency and Productivity Improvements in Surface Irrigation Systems. *Agronomy* **2020**, *10*, 1759. [CrossRef]
50. Moeys, J. Soiltexture: Functions for Soil Texture Plot, Classification and Transformation. 2018. Available online: https://CRAN.R-project.org/package=soiltexture (accessed on 27 December 2022).
51. Donatelli, M.; Wösten, J.H.M.; Belocchi, G. Methods to Evaluate Pedotransfer Functions. *Dev. Soil Sci.* **2004**, *30*, 357–411. [CrossRef]
52. Schaap, M.G. Accuracy and Uncertainty in PTF Predictions. *Dev. Soil Sci.* **2004**, *30*, 33–43. [CrossRef]
53. Zhang, Y.; Schaap, M.G. Estimation of Saturated Hydraulic Conductivity with Pedotransfer Functions: A Review. *J. Hydrol.* **2019**, *575*, 1011–1030. [CrossRef]
54. Trejo-Alonso, J.; Quevedo, A.; Fuentes, C.; Chávez, C. Evaluation and Development of Pedotransfer Functions for Predicting Saturated Hydraulic Conductivity for Mexican Soils. *Agronomy* **2020**, *10*, 1516. [CrossRef]

55. R Core Team. *R: A Language and Environment for Statistical Computing*; R Foundation for Statistical Computing: Vienna, Austria. 2022. Available online: https://www.R-project.org/ (accessed on 27 December 2022).
56. Fritsch S.; Guenther, F.; Wright, M.N. Neuralnet: Training of Neural Networks. R Package Version 1.44.2. 2019. Available online: https://CRAN.R-project.org/package=neuralnet (accessed on 27 December 2022).
57. Kuhn, M. Caret: Classification and Regression Training. R Package Version 6.0-93. 2022. Available online: https://CRAN.R-project.org/package=caret (accessed on 27 December 2022).